

Received November 19, 2018, accepted December 5, 2018, date of publication January 14, 2019, date of current version February 12, 2019.

Digital Object Identifier 10.1109/ACCESS.2019.2892808

# The Impact of Math Anxiety on Working Memory: A Cortical Activations and Cortical Functional Connectivity EEG Study

MANOUSOS A. KLAOS<sup>1,2</sup>, (Member, IEEE), EVANGELOS PARASKEVOPOULOS<sup>2</sup>,  
NIKI PANDRIA<sup>2</sup>, AND PANAGIOTIS D. BAMIDIS<sup>1,2</sup>, (Member, IEEE)

<sup>1</sup>Department of Biomedical Engineering, School of Life and Health Sciences, Aston University, Birmingham B4 7ET, U.K.

<sup>2</sup>Laboratory of Medical Physics, Group of Applied and Affective Neuroscience, Faculty of Health Sciences, Medical School, Aristotle University of Thessaloniki, 54124 Thessaloniki, Greece

Corresponding author: Manousos A. Klados (m.klados@aston.ac.uk)

The work of M. A. Klados was supported in part by the Research Committee, Aristotle University of Thessaloniki.

**ABSTRACT** Mathematical anxiety (MA) is defined as a feeling of tension, apprehension, or fear that interferes with mathematical performance in various daily or academic situations. Cognitive consequences of MA have been studied a lot and revealed that MA seriously affects solving the complex problem due to the corruption of working memory (WM). The corruption of WM caused by MA is well documented in behavioral level, but the involved neurophysiological processes have not been properly addressed, despite the recent attention drawn on the neural basis of MA. This is the second part of our study that intents to investigate the neurophysiological aspects of MA and its implications to WM. In the first study, we saw how MA affects the early stages of numeric stimuli processes as the WM indirectly using event-related potentials in scalp electroencephalographic (EEG) signals. This paper goes one step further to investigate the cortical activations, obtained by the multichannel EEG recordings as well as the cortical functional networks in three WM tasks with increasing difficulty. Our results indicate that the high-math anxious (HMA) group activated more areas linked with negative emotions, pain, and fear, while the low-math anxious (LMA) group activated regions related to the encoding and retrieval processes of the WM. Functional connectivity analysis also reveals that the LMAs' brain has got more structured cortical networks with increased connectivity in areas related to WM, such as the frontal cortex, while the HMAs' brain has a more diffused and unstructured network, superimposing the evidence that the structured processes of WM are corrupted.

**INDEX TERMS** Mathematical anxiety, math anxiety, working memory, EEG, cortical functional connectivity.

## I. INTRODUCTION

Cognitive consequences of mathematical anxiety (MA) have been studied and reviewed by Ashcraft and Ridley [1], who found that MA seriously affects complex problem solving (two-digit mental calculations). Although MA does not affect the retrieval of basic mathematical concepts and calculation strategies, which are stored in long-term memory [2], it seems to affect complex calculations via working memory's (WM) corruption [1]. The correlation of MA to WM corruption has been well documented in a behavioral level [3], but not so deeply in a neurophysiological level.

Only recently, attention was drawn on the neural basis of MA. A fMRI study [4], revealed that math anxious activate regions related to pain perception in the anticipation of mathematical processing, while Young *et al.* [5] support

that MA activates regions that regulate negative emotions. Another recent study, using voxel-based morphometry found that increased MA was associated with reduced grey matter in the left anterior intraparietal sulcus, a region that was also associated with attention, suggesting that baseline differences in morphology may underpin attentional differences between children with low and high MA [6]. Moreover, an electroencephalographic (EEG) study [7] has revealed the relationship among the arithmetic split effect [8] and the P600/P3b component which was more enhanced and delayed in math anxious, while P3 also seems to be modulated by buying decisions in math anxious [9].

In addition to the aforementioned studies, our group has found that MA is related with lower Event Related Potentials (ERPs), during the early stages of the processing

of numeric stimuli [10], while math anxious individuals have a strong effect on the connectivity pattern of brain regions responsible for WM task performances [11]. Moreover, we have also checked the cortical networks during the anticipation of doing mathematics, where we found that anticipatory anxiety prior to mathematical tasks affects so the integration as the segregation of cortical networks [12]. Nevertheless, we need to investigate further the underlying mechanism of how MA corrupts WM while, in addition, relevant functional connectivity issues remain largely unexplored.

This piece of work intents to investigate the neurophysiological aspects of MA and its implications for WM. EEG was used to investigate cortical activations as well as the cortical functional networks in WM task of increasing difficulty that includes trivial numerical stimuli. We hypothesized that when undertaking WM tasks, math anxious, when compared to non-math anxious controls, would show stronger activations in areas linked with negative emotions, pain and fear, such as the Anterior Cingulate Cortex (ACC), Insula and Supplementary Motor Area (SMA) [4], [13], while controls would show stronger activations in areas linked with WM [14], [15].

## II. MATERIALS AND METHODS

### A. PARTICIPANTS

One thousand students of the Aristotle University of Thessaloniki have completed the Abbreviated Math Anxiety Scale (AMAS) [16], which was translated and adapted for the Greek population. AMAS was chosen as due to its relatively short length (9 items only) and its test-retest reliability, while it's correlation with the 98-item long Math Anxiety Rating Scale (MARS) [17] goes up to 0.85 [18]. Two (2) groups of sixteen participants each, were formed from this pool of data, namely LMA (Low Math Anxiety), and HMA (High Math Anxiety) according to their AMAS scores (Figure 1) (AMAS score: LMA:  $11.937 \pm 1.691$  HMA:  $32.875 \pm 3.964$ ;  $F=4.17$   $p<1.52E-18$ ), while controlling other factors, like age, gender, education and dominant hand (equal numbers

of males/females in each group; mean ages were  $22.5 \pm 2.3$  (LMA) and  $22.21 \pm 2.43$  (HMA) -  $p=1$ ). In order to assess their mathematical abilities, we have ranked their school according to how many mathematical courses they have, while ranking scaled from zero (school of literacy) to five (school of mathematics). One-way ANOVA showed that there is not any statistically significant difference ( $F=4.17$ ,  $p=0.26$ ) in the mathematical ability of our groups (LMA:  $2.93 \pm 1.12$ ; HMA:  $2.31 \pm 1.88$ ). Participants with a history of psychiatric or neurological disorder or under medication were excluded from the study. All participants had normal (10/10) or corrected to normal vision. Participants were asked to avoid alcohol intake on the day before and caffeine consumption on the day of the experiment; they were also asked to sleep as adequately and comfortably as possible on the night before. All recordings were performed in a fixed morning slot. All participants signed an informed consent form, while the experimental protocol was approved by the Bioethics committee of the Medical School at the Aristotle University of Thessaloniki, and the study was conducted in accordance to the Declaration of Helsinki.

### B. BEHAVIORAL INDICES

Two behavioral indices were employed to assess participant performance, as proposed by current literature [1]. The first one measures the correctness of the given answers, and it was computed by the means of the d'prime index [19], while the second one measures the reaction time and it was extracted by the stimuli presentation software.

In order to measure the anxiety of our groups we performed STAI I (State Anxiety) and II (Trait Anxiety) tests [20], [21]. STAI I refers to how a person is feeling at the time of a perceived threat and is considered temporary, while STAI II can be defined as feelings of stress, worry, discomfort, etc. that one experiences on a daily basis.

### C. EEG RECORDINGS AND PRE-PROCESSING

EEG recordings were performed in a dark and sound attenuated room. Participants were seated in a comfortable chair and the stimuli were presented on a monitor located about 80 cm in front of the subjects' nasion. EEG signals were recorded with 57 electrodes placed on the scalp according to the 10/10 international system (Fp1, Fp2, F3, F4, C3, C4, P4, O1, O2, F7, F8, T7, T8, P7, P8, Fz, Cz, Pz, TP8, Afz, FCz, CPz, FC1, FC2, CP1, CP2, FC5, FC6, CP5, CP6, Fpz, Oz, F1, Poz, F2, C1, C2, P1, P2, AF3, AF4, FC3, FC4, CP3, CP4, PO3, PO4, F5, F6, C5, C6, P5, P6, FT7, FT8, TP7). Electrodes A1 and A2 served as the reference, while the linked earlobes montage was used. Four ocular electrodes were used; two positioned in the outer canthi of each eye and another two above and below the left eye. The difference of the first couple used to form a bipolar signal for the horizontal electrooculogram (EOG), while the difference of the last two electrodes formed a bipolar signal for the vertical EOG. The signals were amplified and digitized at 500 Hz, while the electrodes' resistance was  $< 2k\Omega$ .

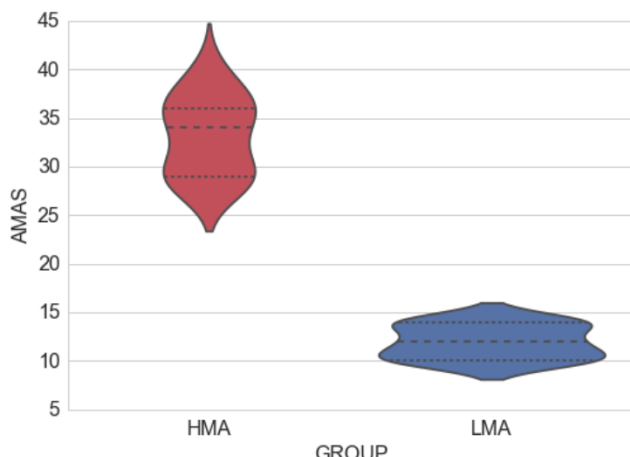


**FIGURE 1.** Violin plots of AMAS scores of both groups, where it is obvious that there is a clear distinction between the two groups' distribution.

During pre-processing, EEG signals were filtered between 0.5–45Hz while the EEGLAB's [22] notch filter was applied in 47–53Hz to remove the line's noise. The REG-ICA methodology [23], [24] was applied to remove ocular artifacts. This methodology was preferred as it removed EOG artifacts while leaving EEG signals relatively intact [24]. According to REG-ICA, extended-ICA [25] was used to decompose EEG signals into independent components (ICs). Subsequently, the algorithm proposed by Schlögl *et al.* [26] was used to filter out the contaminated ICs only, and finally, all the ICs (cleaned or not) were used to reconstruct the cleaned EEG signals. Bad channels were interpolated using the interpolation algorithm included in the EEGLAB software [22], while as a final step three independent expert observers checked EEG signals and removed any bad trials.

#### D. STIMULI AND TASKS

To examine the correlation of MA with WM the n-back task [27] was used in three levels: in the 1-Back Test (BT1-40 trials), participants were asked to press the right mouse-button, if the presented number was the same as the one shown previously, or the left one otherwise. Similarly, in the 2-Back Test (BT2-40 trials) (and 3-Back Test (BT3-40 trials)) subjects had to press the mouse-button if the presented number was the same with the number appeared two (three) positions before (Figure 2). The correspondence of the (true/false) answers to (left/right) mouse-buttons was counterbalanced across subjects for each group separately, while it was kept constant across all tasks for a single subject. The stimuli were randomly presented to each participant, while the EEG was synchronized to the stimulus presentation via a photo resistor adjusted at the lower left corner of the stimulus presentation monitor.

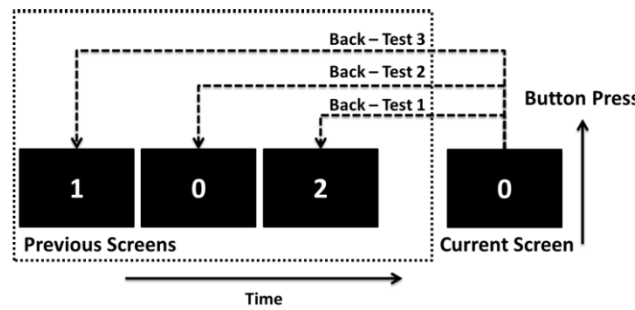


**FIGURE 2.** Tasks used in this study, presented items that were compared with previous (passed) items which should supposedly be stored in WM. Participants had to press the button corresponding to TRUE, if the presented item was the same with the item shown before one (BT1), two (BT2) or three (BT3) trials away, or the other button otherwise. In the presented example, only in BT2, participants should press the button corresponds to TRUE, while for BT1 and BT3 the FALSE button should be pressed.

#### E. CORTICAL ACTIVITY

The Boundary Element Model method (BEM) as implemented within the Brainstorm toolbox [28] was used to compute a generic head model, comprised of four compartments

(scalp, outer and inner skull, cortex) on the basis of an average MRI reconstructed from 152 normal MRI scans (MNI template <http://www.bic.mni.mcgill.ca/ServicesAtlases/ICBM152NLin2009>). BEM compartments were computed by a closed triangle mesh with 4 mm triangle side length and 302 nodes.

Current density reconstructions (CDRs) were calculated on the averaged, over trials, neural responses of each subject for each task (i.e. BT1, BT2, BT3) using sLORETA [29]. sLORETA directly computes a current distribution throughout the full gray matter volume instead of a limited number of dipolar point sources or a distribution restricted to the surface of the cortex, while it has zero error localization even for dipoles included in cortical and non-connected subcortical grey matter [29]. Three separate time windows centered at 200, 300 and 400ms (i.e. T1:180 – 220 ms; T2:280-320 ms; and T3:380-420 ms) were chosen for the CDRs, as driven by the observation of the group differences on the grand average of the corresponding Global Field Power (GFP) (Figure 3 [10]). Only these three fixed time windows were chosen because each one is related to a specific Event Related Potential (ERP) component, while all of them are strongly connected with the mathematical processing [10], [30]–[33].

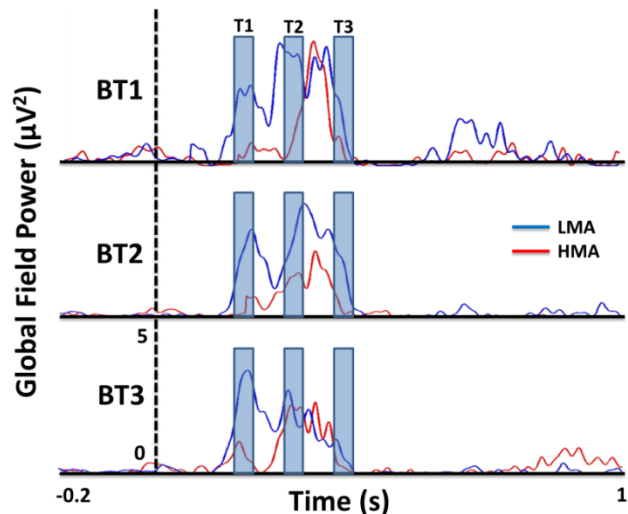


**FIGURE 3.** Global field power (GFP) of the grand average trials of each group. Time window choices are marked by rectangle areas. Note that the LMA group has stronger activity in all tasks, with the most prominent difference in tasks BT1 and BT2, but BT3, which was too hard for both groups anyway. This figure explains our time window choice. Figure is already presented in [10].

Statistical Parametric Mapping 8 (SPM8, <http://www.fil.ion.ucl.ac.uk/spm>) and GLM-Flex ([http://nmr.mgh.harvard.edu/harvardagingbrain/People/AaronSchultz/GLM\\_Flex.html](http://nmr.mgh.harvard.edu/harvardagingbrain/People/AaronSchultz/GLM_Flex.html)) running on Matlab (Math Works Inc., Natick, MA, USA) were used for the statistical analysis of the CDRs. Specifically, using GLM-Flex a separate analysis was designed for each time-window employing a  $2 \times 3$  mixed model ANOVA with the group category (LMA and HMA) as the between subject factor and the BT tasks (BT1; BT2 and BT3) as the within subject factor.

Results were constrained in gray matter using a mask, thereby keeping the search volume small and in physiologically reasonable areas. False Discovery Rate (FDR) correction was adopted in order to control for Type I error, while maintaining the nominal alpha level to .05, except otherwise mentioned. Visualization of the statistical parametric maps was done using MRIcron (<http://www.mccauslandcenter.sc.edu/mricro/mricron/>).

#### F. CORTICAL FUNCTIONAL CONNECTIVITY

EEG records the activity of the cortical sources oriented in tangential or radial directions with respect to the scalp surface. Despite that, the variation of the electrical conductivity among the different head compartments leads to the volume conduction problem, which forms a serious drawback for functional connectivity analysis. To overcome this problem, we have also performed the functional connectivity analysis on the cortical layer. More precisely we have multiplied the inversion kernel extracted by sLORETA [302x57] with our EEG signals averaged over trials [57x1000], thereby obtaining the cortical signals on the nodes of the cortex, as denoted by the triangular mesh extracted by the BEM [34]–[36]. The first 400ms after the stimulus onset were chosen for the extraction of the herein presented functional networks.

A weighted graph is a mathematical object consisting of a set of elements (nodes) that may be linked through binary or weighted connections (edges). In this study, the nodes correspond to the position of the estimated cortical dipoles, while the weight of each edge is given by the Magnitude Square Coherence (MSC) value within each pair of vertices. For this purpose we have used the MSC function of MATLAB (The MathWorks Inc.) with a 50% overlap, based on recent evidence that this is more suitable to model cerebral EEG networks as compared to other connectivity metrics [37]. The MSC in a particular frequency  $f$ , is defined as the square of the cross Power Spectrum Density (PSD) of signals  $x$  and  $y$  divided by the product of the PSDs of  $x$  and  $y$  respectively, as shown by formula (1):

$$MSC_{xy}(f) = \frac{|P_{xy}(f)|^2}{P_{xx}(f)P_{yy}(f)} \quad (1)$$

PSD was estimated using the Welch method [38]. Signals between 0-400msec were divided into segments containing 40 samples each, and PSD was then computed using formula (2):

$$P(f) = \frac{1}{f_s L_s U} \int_{-\frac{f_s}{2}}^{\frac{f_s}{2}} D_{xx}(\rho) |W(f - \rho)|^2 d\rho \quad (2)$$

In this formula,  $D_{xx}$  is the Discrete Fourier Transform of the signal's correlation sequence  $R_{xx}$ ,  $f_s$  is the digitization rate (500 Hz in this case),  $L_s$  is the segment length and  $U$  is a normalization constant ensuring that the PSD is asymptotically unbiased. This process leads to 96 [16 subjects \* 6 frequency bands: delta (0.5-4Hz), theta (4-8Hz),

alpha1 (8-10Hz), alpha2 (10-12Hz), gamma (30-45Hz)] fully connected graphs for each group, for each task separately. A threshold to 0 was applied to each graph, isolating all negative weights. To investigate the impact of MA into the network structure the following parameters were employed:

#### 1) DENSITY (DEN)

graph density indicates how many edges are inside the graph divided by the maximum possible number of edges between the vertices of the graph. This definition is only used for binary (not weighted) graphs, so it was adapted herein to fit our needs. We define the density of a weighted network as the sum of all weights divided by the maximum possible number of edges between the vertices multiplied by the maximum value of the current connectivity metric (MSC in this case), as shown in formula (3):

$$DEN = \frac{\sum_{W_{ij} \in G \wedge i \neq j} W_{ij}}{(V(V-1))max(MSC)} = \frac{\sum_{W_{ij} \in G \wedge i \neq j} W_{ij}}{(V(V-1))} \quad (3)$$

where  $V$  denotes the number of nodes.

#### 2) CLUSTERING COEFFICIENT (CC)

it denotes the fraction of triangles around a node is equivalent to the fraction of node neighbors that are neighbors of each other. There are at least four different definitions [39] regarding the computation of the weighted clustering coefficient. For the purposes of the current analysis we used the definition proposed by [40] (see formula (4)) as it takes into account the weights of all edges in a triangle and it is invariant to the weights permutation in a single triangle:

$$\widehat{C}_i = \frac{2}{k_i(k_i - 1)} \sum_{j \neq k} (\widehat{w}_{ij}\widehat{w}_{jk}\widehat{w}_{ki})^{1/3} \quad (4)$$

where  $k_i$  denotes the node strength of the  $i^{\text{th}}$  node and  $\widehat{w}_{ij}$  is the normalized weight of the edge connecting the  $i^{\text{th}}$  and  $j^{\text{th}}$  nodes.

#### 3) CHARACTERISTIC PATH LENGTH (CPL)

The characteristic path length is the average shortest path length in the network.

#### 4) GLOBAL MODULARITY (GM)

The optimal community structure is a subdivision of the network into non-overlapping groups of nodes in a way that maximizes the number of within-group edges and minimizes the number of between-group edges. GM is a statistic that quantifies the degree to which the network may be subdivided into such clearly delineated groups. GM used was proposed by [41] and it is also implemented in the Brain Connectivity Toolbox for MATLAB [42]. After identifying the partition of the network, we measured the overall number of modules (NUM). Additionally we quantified some nodal characteristics, like the intra- and inter-module connectivity [43], [44]. The first one is measured by means of the within-module degree z-score (Z) (5), while the second one by the

Participation Coefficient (PC) (6).

$$Z_i = \frac{k_i - \bar{k}_{s_i}}{\sigma_{k_{s_i}}} \quad (5)$$

$$PC_i = 1 - \sum_{s=1}^{n_M} \left( \frac{\bar{k}_{s_i}}{k_i} \right)^2 \quad (6)$$

In both formulas  $k_i$  denotes the node strength of the  $i^{\text{th}}$  node in the  $s_i$  module,  $\bar{k}_{s_i}$  is the mean strength of the  $s_i$  module, and  $\sigma_{k_{s_i}}$  is the standard deviation of the  $k_{s_i}$ .

### 5) BETWEENNESS CENTRALITY (BC) AND EDGE BETWEENNESS CENTRALITY (EBC)

BC is a measure of a node's centrality in a network. It is equal to the number of shortest paths from all vertices to all others that pass through that node, while EBC is exactly the same apart from its application to edges instead of nodes. In this analysis, we used the algorithm proposed by [45] for the computation of BC and EBC.

### 6) SMALL-WORLD INDEX (S)

A small-world network is a graph in which most nodes are not neighbors of one another, but most nodes can be reached from every other in a small number of steps. Humphries and Gurney [46] have defined the S of a network as:

$$S = \frac{C/C_{\text{rand}}}{L/L_{\text{rand}}} \quad (7)$$

where C, L are the CC and the short path length respectively, whereas the  $C_{\text{rand}}, L_{\text{rand}}$  indices define the mean values of C and L respectively, as extracted by fifty surrogate random networks. Each random network was produced by a random rewiring of the observed network [47].

All graph parameters, with exception of SWN, are implemented within the Brain Connectivity Toolbox for MATLAB [42]. Similarly, to the statistical analysis of the cortical activations, the analysis used for the graph parameters was a  $2 \times 3$  mixed model ANOVA with the group category (LMA, HMA) being the between-subject factor and the tasks (BT1, BT2, BT3) being the within-subject factor. Only for the nodal characteristics (Z, PC, BC, EBC) we have used pairwise t-tests for each node separately. False Discovery Rate (FDR) was also adopted herein in order to control for Type I errors, while maintaining the nominal alpha level to .05. The statistical analysis of the graph parameters was performed in SPSS v.20.

## III. RESULTS

### A. BEHAVIORAL DATA

In addition to MA differences between our groups (Figure 1), HMA group reported also higher situational anxiety ( $t(30) = 3.94, p = 0.0001$ ), compared to LMA, while both groups have comparable levels of trait anxiety ( $p > 0.10$ ). The Pearson correlation between AMAS and state anxiety was moderate ( $r = 0.575, p = 0.001$ ) and much lower between AMAS and trait anxiety ( $r = 0.274, p = 0.129$ ) in accordance with the original standardization study of AMAS [48].

Regarding the behavioral indices mentioned above, we didn't find any Group  $\times$  Task interaction ( $p > 0.7$ ). However, pairwise comparisons exhibited that Group effect on d'prime was significant only during the BT3 [10].

### B. CORTICAL ACTIVATION – T1 TIME WINDOW

The statistical analysis of the CDRs in the T1 time-window showed no significant result in the interaction of Group  $\times$  Task indicating that the three levels of the BT tasks affected the two groups equally. Nevertheless, a significant main effect of Group indicated that there were significant differences in the cortical activity of the two groups, independently of the BT task. Specifically, the main effect of group revealed that the HMA group had significantly greater activity than the group of LMA in one cluster located in the left middle temporal gyrus (MTG) [peak coordinates:  $x = -55, y = 4, z = -21$ ;  $t(30) = 6.19$ ; cluster size = 90 voxels;  $p < 0.05$  FDR corrected] (Figure 5).

On the other hand, LMA had significantly greater activity in 4 clusters: one located in the right superior frontal gyrus (SFG) [peak coordinates:  $x = 10, y = 48, z = 44$ ;  $t(30) = -5.3450$ ; cluster size = 222 voxels;  $p < 0.05$  FDR corrected], one located in the right middle frontal gyrus (MFG) [peak coordinates:  $x = 34, y = 50, z = 18$ ;  $t(30) = -4.7207$ ; cluster size = 572 voxels;  $p < 0.05$  FDR corrected], one located in the left inferior frontal gyrus (IFG) [peak coordinates:  $x = -57, y = 28, z = 2$ ;  $t(30) = -3.6289$ ; cluster size = 133 voxels;  $p < 0.05$  FDR corrected], and one located in the left postcentral gyrus (PCG) [peak coordinates:  $x = -39, y = -31, z = 70$ ;  $t(30) = -3.7784$ ; cluster size = 112 voxels;  $p < 0.05$  FDR corrected]. Statistical maps of this analysis are presented in Figure 4 (all anatomical regions were defined using the AAL atlas [49]).

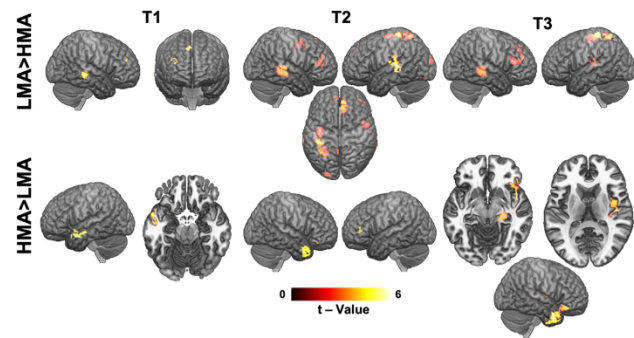


**FIGURE 4.** Statistically significant differences among the two groups in all three-time windows. LMA group activate more areas of the frontal, temporal and parietal cortex, which are linked with WM processes. On the other hand, HMA group activate more areas like the pole of the right MTG, the insula and the parahippocampal gyrus, which are connected to negative emotions, pain and fear.

### C. CORTICAL ACTIVATION – T2 TIME WINDOW

The statistical analysis of the CDRs in the T2 time-window showed a significant interaction of Group  $\times$  Task indicating that the group difference was differentially affected by the

**TABLE 1.** Summarized results for the group × task interaction effect in T2 time window.

Location of activation	Peak voxel t-value	Hem	Coordinates			Cluster Size
			X	Y	Z	
Parahippocampal Gyrus	8.76	L	-27	-37	-7	101
Parahippocampal Gyrus	6.43	R	18	-27	-9	117
Middle Frontal Gyrus	10.94	L	-41	48	-13	231
Superior Frontal Gyrus	10.51	L	-15	58	-9	51
Superior Temporal Gyrus	7.93	R	48	-21	2	62
Superior Temporal Gyrus	12.03	L	-46	-37	15	131
Middle Frontal Gyrus	13.29	R	8	46	44	1903

**TABLE 2.** Summarized results for the group × task interaction effect in T3 time window.

Location of activation	Peak voxel t-value	Hemisphere	Coordinates			Cluster Size
			X	Y	Z	
Inferior frontal gyrus	13.74	R	20	16	-23	1262
Fusiform gyrus	12.25	L	-31	-47	-21	171
Hippocampal gyrus	15.97	L	-25	-39	-1	182
Parahippocampal gyrus	7.82	R	26	-35	-7	63
Posterior cingulate gyrus	8.68	L	-11	-57	-1	186
Superior temporal gyrus	7.89	L	-63	-37	8	203
Middle occipital gyrus	8.24	R	22	-97	4	65
Inferior frontal gyrus	7.1	L	-43	0	8	132
Cuneus	8.33	L	-13	-38	10	82
Inferior frontal gyrus	9.5	R	38	18	28	148
Supramarginal gyrus	9.86	R	46	-33	44	1580
Cuneus	9.46	R	12	-83	40	140
Posterior cingulate gyrus	10.09	R	4	-83	46	1059
Inferior parietal gyrus	11.82	L	-37	-45	50	337
Middle frontal gyrus	11.29	R	40	18	46	493
Postcentral gyrus	10.78	L	-41	-33	56	292
Middle frontal gyrus	7.01	L	-23	10	68	145

3 levels of BT. This interaction effect was located mainly in prefrontal, temporal and cingulate regions (the complete list of clusters is presented in Table 1). In order to resolve this two-way interaction, three post-hoc independent samples t-tests were performed (i.e. one for BT1, one for BT2 and one for BT3) using the interaction effect as a localizer; the results of the post-hoc analyses were restricted to the cortical regions, where the two-way interaction was found to be significant.

The independent samples t-test for BT1 revealed that the group of LMA had significantly greater activity than the group of HMA in 6 clusters: one located in IFG [peak coordinates:  $x = -55$ ,  $y = 32$ ,  $z = -5$ ;  $t(60) = -5.42$ ; cluster size = 65 voxels;  $p < 0.05$  FDR corrected], one located in the left hippocampal gyrus (HG) [peak coordinates:  $x = -25$ ,  $y = -37$ ,  $z = -3$ ;  $t(60) = -4.52$ ; cluster size = 85 voxels;  $p < 0.05$  FDR corrected], one located in the left superior temporal gyrus (STG) [peak coordinates:  $x = -45$ ,  $y = -41$ ,  $z = 22$ ;  $t(60) = -3.83$ ; cluster size = 74 voxels;  $p < 0.05$  FDR corrected], one in the right SFG [peak coordinates:  $x = 2$ ,  $y = 28$ ,  $z = 48$ ;  $t(60) = -9.83$ ; cluster size = 1688 voxels;  $p < 0.05$  FDR corrected], one in the posterior parietal cortex (PPC) [peak coordinates:  $x = -13$ ,  $y = -49$ ,  $z = 64$ ;  $t(60) = -5.95$ ; cluster size = 238 voxels;  $p < 0.05$  FDR

corrected], and one located in the right MFG [peak coordinates:  $x = 20$ ,  $y = -25$ ,  $z = -9$ ;  $t(60) = -5.68$ ; cluster size = 110 voxels;  $p < 0.05$  FDR corrected]. In contrast the group of HMA did not show significantly greater activity than the LMA group in BT1.

Similarly to the results of the BT1, the independent samples t-test for BT2 revealed that the group of LMA showed significantly greater activity in two clusters: both of them located in the right SFG [peak coordinates for cluster (a):  $x = 34$ ,  $y = 50$ ,  $z = 18$ ;  $t(60) = -4.74$ ; cluster size = 465 voxels; peak coordinates for cluster (b):  $x = 2$ ,  $y = 30$ ,  $z = 48$ ;  $t(60) = -5.20$ ; cluster size = 127 voxels;  $p < 0.05$  FDR corrected] (Figure 5). Again, the HMA group did not show significantly greater activity than the LMA group.

In contrast to the previous two t-tests, the independent samples t-test for BT3 revealed that the group of LMA did not show significantly greater activity than the HMA group. Instead, the group of HMA showed significantly greater activity in 6 clusters: one located in right parahippocampal gyrus (PHG) [peak coordinates:  $x = 20$ ,  $y = -25$ ,  $z = -9$ ;  $t(60) = 3.69$ ; cluster size = 105 voxels;  $p < 0.05$  FDR corrected], one located in the left MFG [peak coordinates:  $x = -39$ ,  $y = 50$ ,  $z = 13$ ;  $t(60) = 4.77$ ; cluster size = 68 voxels;

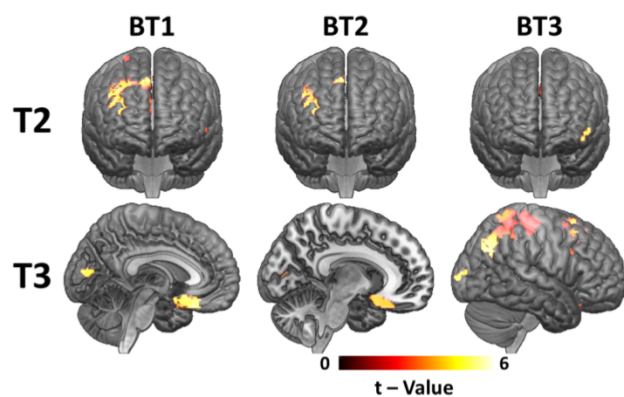


**FIGURE 5.** Localized areas where there is a statistically significant difference among the cortical activations between LMA and HMA groups for all three tasks in T2 and T3 time windows. Note that for BT1 and BT2 tasks, LMA has greater activity in the depicted areas, while in BT3, HMA group has significantly greater activity as it is shown in the next section.

$p < 0.05$  FDR corrected], one located in the right STG [peak coordinates:  $x = 47, y = -19, z = 2$ ;  $t(60) = 4.69$ ; cluster size = 61 voxels;  $p < 0.05$  FDR corrected], one located in the left STG [peak coordinates:  $x = -39, y = -29, z = 8$ ;  $t(60) = 3.74$ ; cluster size = 59 voxels;  $p < 0.05$  FDR corrected], one located in the anterior cingulate cortex (ACC) [peak coordinates:  $x = 8, y = 24, z = 24$ ;  $t(60) = 3.99$ ; cluster size = 80 voxels;  $p < 0.05$  FDR corrected], and one located in the posterior cingulate cortex (PCC) [peak coordinates:  $x = -1, y = -87, z = 38$ ;  $t(60) = 4.48$ ; cluster size = 75 voxels;  $p < 0.05$  FDR corrected] (Figure 6).

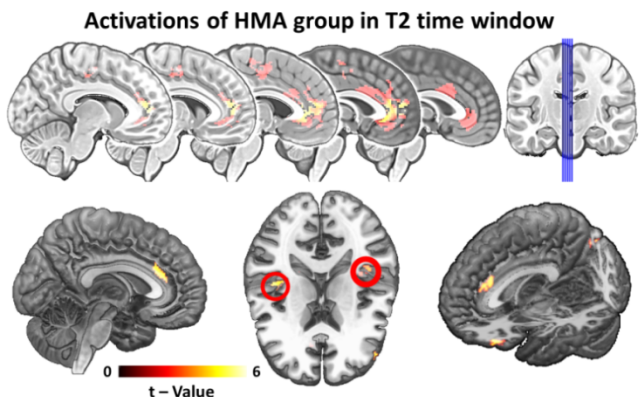


**FIGURE 6.** Illustration of areas where HMA have significantly greater activity in the T2 time window. (Top) areas extracted by the main effect of Group; note that HMA group has significantly greater activity in the ACC, as well as, in the supplementary motor area (SMA). (Bottom) results of the Group x Task interaction. HMA has significantly greater activity in the ACC and (bilaterally) in Insula.

The independent samples t-test for BT1 revealed that the group of LMA had significantly greater activity than the group of HMA in 3 clusters: one located in the left MFG [peak coordinates:  $x = 18, y = 18, z = -25$ ;  $t(60) = -4.55$ ; cluster size = 825 voxels;  $p < 0.05$  FDR corrected], one located in the left SFG [peak coordinates:  $x = -65, y = -37$ ,

$z = 6$ ;  $t(60) = -4.04$ ; cluster size = 69 voxels;  $p < 0.05$  FDR corrected] and one located in the left cuneus [peak coordinates:  $x = -15, y = -81, z = 10$ ;  $t(60) = -4.48$ ; cluster size = 81 voxels;  $p < 0.05$  FDR corrected] (Figure 5). The group of HMA did not show significantly greater activity in any area than the LMA group in BT1.

The independent samples t-test for BT2 revealed that the group of LMA had significantly greater activity than the group of HMA in 3 clusters: one in the right MFG [peak coordinates:  $x = 6, y = 12, z = -21$ ;  $t(60) = -3.43$ ; cluster size = 258 voxels;  $p < 0.05$  FDR corrected], one located in the left cuneus [peak coordinates:  $x = -3, y = -87, z = 10$ ;  $t(60) = -4.80$ ; cluster size = 81 voxels;  $p < 0.05$  FDR corrected], and one in the left inferior parietal gyrus (IPG) [peak coordinates:  $x = -39, y = -33, z = 60$ ;  $t(60) = -4.36$ ; cluster size = 194 voxels;  $p < 0.05$  FDR corrected] (Figure 5). The group of HMA did not show significantly greater activity in any area than the LMA group in BT2.

In contrast to the previous two t-tests, the independent samples t-test for BT3 revealed that the group of LMA did not show significantly greater activity than the HMA group. Instead, the group of HMA showed significantly greater activity in 8 clusters: one located in the left PHIG [peak coordinates:  $x = -15, y = -29, z = -9$ ;  $t(60) = 5.04$ ; cluster size = 100 voxels;  $p < 0.05$  FDR corrected], one located in the middle occipital gyrus (MOG) [peak coordinates:  $x = 22, y = -101, z = -2$ ;  $t(60) = 6.06$ ; cluster size = 65 voxels;  $p < 0.05$  FDR corrected], one located in the left Insula [peak coordinates:  $x = -47, y = 4, z = 6$ ;  $t(60) = 4.39$ ; cluster size = 118 voxels;  $p < 0.05$  FDR corrected], one located in the right IFG [peak coordinates:  $x = 38, y = 14, z = 28$ ;  $t(60) = 4.08$ ; cluster size = 104 voxels;  $p < 0.05$  FDR corrected], one located in the right supramarginal gyrus [peak coordinates:  $x = 40, y = -59, z = 32$ ;  $t(60) = 6.34$ ; cluster size = 1334 voxels;  $p < 0.05$  FDR corrected], one located in the posterior cingulate gyrus [peak coordinates:  $x = 6, y = -40, z = 47$ ;  $t(60) = 5.04$ ; cluster size = 61 voxels;  $p < 0.05$  FDR corrected], and one in the right MFG [peak coordinates:  $x = 40, y = 20, z = 48$ ;  $t(60) = 5.22$ ; cluster size = 451 voxels;  $p < 0.05$  FDR corrected] (Figure 5).

#### D. CORTICAL FUNCTIONAL NETWORKS

CPL and NUM didn't show any statistically significant differences, so they are excluded from further reporting, which concentrates into those parameters indicating alterations to network organization and structure due to MA. These results are depicted below in Figure 7.

Significant results have been found in CC in both delta ( $F(1;30) = 6.890; p = 0.014$ ) and theta ( $F(1;30) = 4.903; p = 0.035$ ) bands concerning the testing group. More precisely, LMA group seem to have higher clustering performance in the aforementioned bands delta (LMA:  $0.367 \pm 0.020$ , HMA:  $0.292 \pm 0.020$ ), theta (LMA:  $0.366 \pm 0.019$ , HMA:  $0.308 \pm 0.019$ ) than HMA group. This indicates that LMA group shows greater efficiency in their wiring,

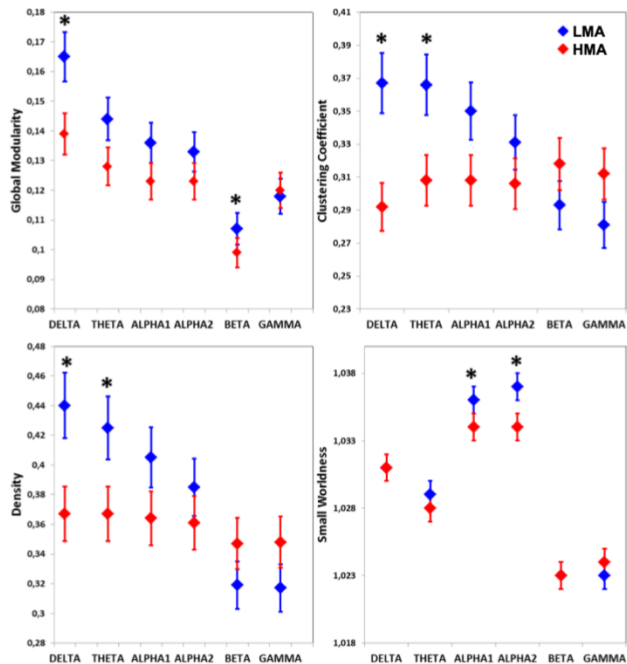


**FIGURE 7.** Network Parameters that appear to have statistically significant differences due to MA. GM (top left) reveals that the network modularity is altered due to MA in delta and beta bands, revealing networks with higher modularity structures for LMA. CC (top right) and DEN (bottom left) have similar patterns, as they are strongly related with each other, and in both LMA has increased values over the delta and theta bands; theta rhythm is strongly related with WM. SWN (bottom right), seems to support that the efficient communication of the network significantly drops in the HMA group in alpha band.

compared to HMA, by increasing the degree to which, nodes tend to cluster together.

Alternations in density were found to be significant in delta ( $F(1;30) = 7.853$ ;  $p = 0.009$ ) and theta ( $F(1;30) = 5.579$ ;  $p = 0.025$ ) bands, where LMA group seems to have higher density (delta: LMA:  $0.440 \pm 0.018$ , HMA:  $0.367 \pm 0.018$ ; theta: LMA:  $0.425 \pm 0.018$ , HMA:  $0.367 \pm 0.018$ ). This is strongly connected with the CC, which also reveals the efficiency of LMA group. It should be noted that theta band is strongly connected with WM. Despite the numerical interpretation of density's results, we can extract some results from the illustration of cortical networks (Figure 8). There is no statistically significant difference among the tasks, so we chose to depict only the networks for BT1 (the graphs of BT2 and BT3 are identical). In Figure 8, we can see that the LMA group forms a clear pattern in all brainwaves which connects the left temporal lobe with the right frontal cortex, while HMA have a more random and chaotic pattern. In the third row of Figure 8 we can see the stronger connections of the difference among LMA and HMA groups, where the aforementioned pattern is enhanced.

The main effect of group in the networks' SWN showed that MA affects the alpha1 ( $F(1;30) = 4.294$ ;  $p = 0.047$ ; LMA:  $1.036 \pm 0.001$ , HMA:  $1.034 \pm 0.001$ ) and alpha2 ( $F(1;30) = 4.627$ ;  $p = 0.041$ ; LMA:  $1.037 \pm 0.001$ , HMA:  $1.034 \pm 0.001$ ) brainwaves. SWN is the main indicator

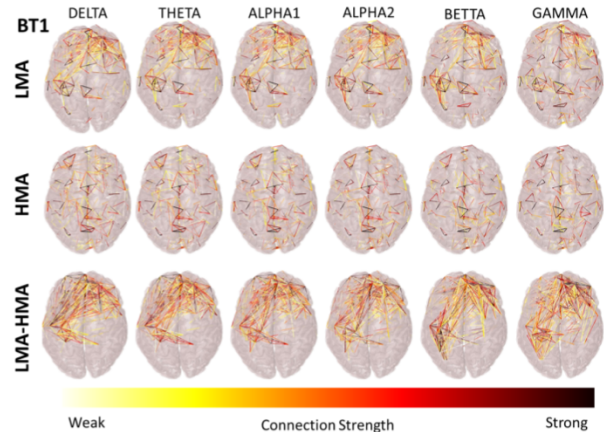


**FIGURE 8.** Functional Connectivity Networks of the two groups, and their differences as well, in our six frequency bands according to the MSC metric. Only the stronger network connections are shown (around 1% (912 edges)). Top row: the LMA group shows a clear pattern connecting the left temporal region with the right frontal cortex. Middle row: the HMA group exhibits a more random and chaotic pattern. Bottom row: the stronger connections (around 1% (912 edges)) of the difference among LMA and HMA groups, where the aforementioned pattern seems to be enhanced.

of the network's efficacy, and according to these results LMA group seems to be more efficient compared to HMA.

The Interaction of Group x Task was found to be marginally significant in GM in delta band ( $F(1;30) = 2.753$ ;  $p = 0.079$ ), while the post-hoc analysis revealed that this was provoked by the BT2 task ( $p = 0.016$ ). The main effect of group was statistically significant in delta ( $F(1;30) = 4.426$ ;  $p = 0.044$ ) and beta bands ( $F(1;30) = 4.905$ ;  $p = 0.035$ ). In both brain bands the LMA group seems to have a higher modular organization as denoted by global modularity (delta: LMA:  $0.139 \pm 0.009$ , HMA:  $0.165 \pm 0.009$ ; beta: LMA:  $0.107 \pm 0.002$ , HMA:  $0.099 \pm 0.002$ ).

Regarding the Z and the PC we should note that although two nodes may have the same z-score, they may play different roles within the cluster. Therefore, this measure is often compared with the PC. Z and PC together reveal whether nodes are truly hubs in the network. Thus, Figure 9 depicts only those nodes that are, for both indices, greater for one group

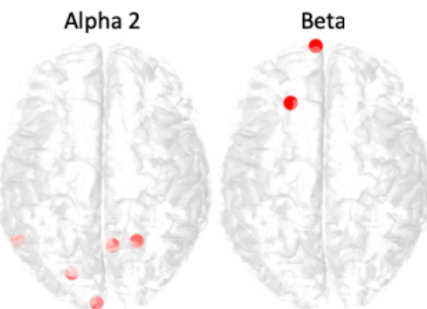


**FIGURE 9.** Nodes that have significantly greater Z and PC values in LMA compared to HMA in BT1.

(in this case LMA), while simultaneously they both have statistically significant differences between the two groups in BT1 task. The rest tasks didn't have nodes that were for both indices significantly different between our two groups. Note that the group of LMA has significantly higher PC and Z in nodes of the parieto-occipital cortex for Alpha2, which is probably linked with the attentional buffer involved in WM, something well documented by [50]. For the Beta band, the LMA group appears to have significantly higher PC and Z in the frontal and prefrontal regions probably due to the encoding of memorized objects [51] as well as to WM related activity [52]. We did not find significant differences for the remaining frequency bands and for any of the other tasks.

Removing a node (edge) with high BC (EBC), we break many short paths, thereby dropping the communication efficacy of the network. In the results presented in Figure 10, the nodes and edges that have statistically significant difference (p-values were corrected with FDR) between the two groups are illustrated: blue (red) denotes nodes/edges with significantly higher BC/EBC for LMA (HMA) group. BC and EBC findings support the CDR findings, by revealing that HMA group have more central nodes in the midline (i.e. ACC and SMA), as well as, in the parietal (i.e. Insula) and occipital cortex (i.e. Cuneus), while the central nodes of LMA are around the left temporal and the right frontal cortex. One can also notice that the EBC appears only in Beta and Gamma band, being denser in the first of the two. It can be also noticed that the LMA group drop their BC and EBC according to task difficulty. This means that LMA have an overall communication efficacy which can support

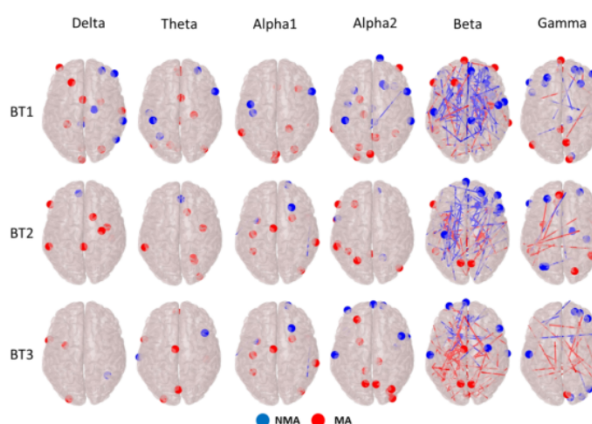


**FIGURE 10.** BC and EBC plots: In this figure we can see the nodes and the edges that have significantly higher BC and EBC respectively. With blue (red) color we denote the nodes/edges which have higher BC/EBC in LMA (HMA) group. We can see that HMA have their central nodes around the midline and the posterior parietal cortex, supporting the CDR findings, while LMA's central nodes are around the left temporal and right frontal cortex, enhancing the pattern revealed from the density's analysis. Regarding the EBC we can clearly observe that they appear mainly in Beta band which is essential for the encoding of memorized objects. The aforementioned LMA's pattern seems to be still unaltered, while it gets weaker across the task's difficulty. This means that the LMA group has a better overall communication's efficacy which can support the internal cognitive processes of WM, and it doesn't depend on certain nodes or edges.

the internal cognitive processes of WM and they do not depend on specific nodes or edges. On the other hand, HMA group increases its BC and EBC alongside with increasing task difficulty, which means that, both the mnemonic and the affective networks are still engaged and reinforced by the increasing demand and the stronger negative emotions respectively.

#### IV. DISCUSSION

Behavioral results reveal a suppression of WM in MA, by showing high reaction time and high error rates for HMA. Both of these findings come in line with current literature [1], where it is supported that although math anxious try to succeed in a certain task (high reaction time), they fail (high error rate) because their anxiety consumes resources of their WM system. It should be mentioned at this point that although state anxiety may play a role in T1, where no Group × Task interaction was found the modulation of our results with the task difficulty in the other time windows, leads to assuming that MA is mainly responsible for these findings.

Our study goes one step further from prior obtained behavioral results and explains this consumption by the means of cortical activations and cortical connectivity. In contrast to LMA, who have stronger activations in areas related to WM tasks, HMA exhibit strong activation in areas included in the pain network like the ACC, the SMA (Figure 7), the Insula and the PHG (Table 1), even by viewing simple numbers. The ACC has been identified as a basic component of the parallel distributed attentional [53] and emotional [54], [55] network, while it has also been found to be activated during negative emotions [54], [55]. Moreover, numerous studies integrate all the aforementioned areas in the perception of pain [56]–[59] which seems to be activated due to hurting past memories as well. The combination of these areas can be further explained by considering the existing relationship of hippocampus with the retrieval of long-term memories, and the involvement of amygdala when this memory recall has an emotional background [13], [60], [61]. More precisely, the ACC and the insula receive signals from the amygdala and hippocampus using the PHG [62]–[64]; thus, they are activated during affective mnemonic functions [13], [65]. Amygdala hyperactivity has also been linked with MA in conjunction with lower problem-solving demands [5]. In the same way, a recent study found that math anxious activate pain related areas in the anticipation of doing mathematics [4]. Our study enhances this theory, by revealing that math anxious also activate pain related areas during a WM task.

A typical working memory task is usually consisted of an initial encoding period, followed by a delay period and finally a retrieval task. LMA show significantly greater activity in areas related to WM [66], something indicating that their WM function seems to be more efficient in contrast to that of HMA. The reported results are in line with our hypothesis, as they indicate an activation of both the left IFG and the right MFG at T1. According to a previous study these two regions were activated during the delay period of a working memory

task [67]. According to the same study, left IFG is also active during the encoding phase, while MFG is found to have increased functional connectivity with the PCC during a WM task [15]. A more recent study provided evidence of right SFG and bilateral PCG during encoding [68]. These regions were also active in our study during T1 and T3 and they are related with processing of information during working memory tasks.

We found also activation in the left cuneus. This region was found in studies employing fMRI while participants performed both operation span and arithmetic tasks [69]. Increased activation of the same area was also demonstrated in another study which employed fifteen participants who practiced for 6 weeks in working memory tasks [70]. We should state cuneus's role during novel stimulus encoding [71]. Cuneus is involved in the phonological representation of the stimuli [72], which is essential for the encoding phase, where the articulatory rehearsal is performed [73]. A recent study [74] connects the phonological processing of WM with increased activity in the supramarginal gyrus.

In modern network theory, the brain is a complex network that evaluates the segregation and integration of functional regions, which seem to be also altered during the anticipatory phase prior doing maths [12]. Our functional connectivity network findings revealed for the LMA group, a frontal activation linked with activation in the left temporal lobe. This pattern is also found by other studies with different modalities (EEG, fMRI, etc.) [14], [15], [75]. More precisely, we can see that the number of intra-connections of the right frontal cortex, as well as, that of the inter-connections among the two aforementioned regions is increased. Considering that both regions are involved in WM [76], [77], this finding superimposes the evidence that WM is corrupted in HMA group, as a more diffused network activation is observed. It is known that WM is negatively affected by acute and chronic stress, due to a decrease of frontal cortex neuronal firing, as a result of the stress-induced catecholamine release [78]. fMRI studies have also linked the reduced WM performance caused by stress with the deactivation of the dorsolateral prefrontal cortex due to increased catecholamine release [79], while the functional connectivity of the frontal cortex seems to be weakened due in stressful situations [80].

In this study, LMA and HMA show also differences in brain organization in both easy and difficult WM tasks. It is interesting that there is a difference between the groups in easy tasks (i.e. BT1) (Figure 8). The network organization of LMA at BT1 differs mainly in low frequency bands, which are believed to have a main role in long-range coordination where local activations occur [81]. Thus, it seems that there is a degree of weaker long coordination in HMA individuals. In contrast, LMA individuals show signs of higher long-distance coordination and the higher CC and DEN are indicative of higher local activations in regions coordinated by the low frequency bands.

Increased activity in Alpha1 and Alpha2 bands is often found during cognitive tasks [82], [83] in combination with

activity in higher frequencies [84]. The increased SWN index in LMA individuals shows a better network organization in contrast to that of HMA individuals. There seems to be a sign of higher readiness to react in cognitive demands, which goes in parallel with our behavioral findings. The higher GM of beta band in LMA individuals could be also explained as higher interregional activity together with the higher role of lower frequency bands. Simultaneously, it can be related to higher SWN index of Alpha1 and Alpha2 bands, while it is probably due to the encoding of memorized objects [51], as well as, due to WM related activity [52].

Admittedly, however, our study does contain some limitations. One of them lies with the experimental setup, in which the use of a motor execution task (mouse button press) does not facilitate a careful observation of what is happening in the pre-stimulus interval, like in the study of [85]. Despite the fact that the motor task was counterbalanced across the subjects of each group and its effect does not appear in the GFP plots (Figure 3), we chose to investigate only the post-stimulus interval, where the ongoing mental activity cannot be corrupted by button presses. Another point that it should be underlined is the relatively low number of trials (40 for each BT). Although more trials enhance the signal to noise ratio and the accuracy of results, they could also introduce mental fatigue of participants accompanied with the well-known behavioral and neurophysiological consequences. A final limitation to note is the use of a generic head model in the performance of CDR analysis. It would be very interesting for future investigations to examine the relationship of MA and WM using individualized head models, in order to specify alternations in exact functional regions.

Despite these limitations, our confirmed hypothesis supports that some resources of WM are consumed due to MA, because math anxious activate mainly regions related with negative emotions and pain, as the energy consumed in areas associated with WM is found to be significantly higher in LMA. This in itself is a very interesting finding considering that none of the used tasks required any mathematical processing, while the numbers used for the Back Tests were trivial. This finding dispute the current studies that use numerical stimuli without controlling the levels of MA, while it further suggests that future studies, which use numerical stimuli, should take math anxiety into account. The obvious significance of this finding cannot be underestimated.

## REFERENCES

- [1] M. H. Ashcraft and K. S. Ridley, "Math anxiety and its cognitive consequences," in *The Handbook of Mathematical Cognition*, J. I. D. Campbell, Ed. New York, NY, USA: Psychol. Press Ltd., 2005, pp. 315–327.
- [2] E. P. Kirk and M. H. Ashcraft, "Telling stories: The perils and promise of using verbal reports to study math strategies," *J. Exp. Psychol. Learn. Memory, Cogn.*, vol. 27, no. 1, pp. 157–175, Jan. 2001.
- [3] K. P. Raghubar, M. A. Barnes, and S. A. Hecht, "Working memory and mathematics: A review of developmental, individual difference, and cognitive approaches," *Learn. Individual Differences*, vol. 20, no. 2, pp. 110–122, Apr. 2010.
- [4] I. M. Lyons and S. L. Beilock, "When math hurts: Math anxiety predicts pain network activation in anticipation of doing math," *PLoS ONE*, vol. 7, no. 10, p. e48076, Jan. 2012.

- [5] C. B. Young, S. S. Wu, and V. Menon, "The neurodevelopmental basis of math anxiety," *Psychol. Sci.*, vol. 23, no. 5, pp. 492–501, May 2012.
- [6] C. E. Hartwright *et al.*, "The neurocognitive architecture of individual differences in math anxiety in typical children," *Sci. Rep.*, vol. 8, no. 1, Dec. 2018, Art. no. 8500.
- [7] M. Suárez-Pellicioni, M. I. Núñez-Peña, and A. Colomé, "Mathematical anxiety effects on simple arithmetic processing efficiency: An event-related potential study," *Biol. Psychol.*, vol. 94, no. 3, pp. 517–526, Dec. 2013.
- [8] M. H. Ashcraft and J. Battaglia, "Cognitive arithmetic: Evidence for retrieval and decision processes in mental addition," *J. Exp. Psychol. Hum. Learn. Mem.*, vol. 4, no. 5, pp. 527–538, 1978.
- [9] W. J. Jones, T. L. Childers, and Y. Jiang, "The shopping brain: Math anxiety modulates brain responses to buying decisions," *Biol. Psychol.*, vol. 89, no. 1, pp. 201–213, Jan. 2012.
- [10] M. A. Klados, P. Simos, S. Micheloyannis, D. Margulies, and P. D. Bamidis, "ERP measures of math anxiety: How math anxiety affects working memory and mental calculation tasks?" *Front. Behav. Neurosci.*, vol. 9, p. 282, Oct. 2015.
- [11] S. Bayrak, D. Margulies, P. Bamidis, and M. A. Klados, "Mathematical Anxiety influences the cortical connectivity profiles in lower alpha band during working memory tasks," *Frontiers Hum. Neurosci.*, vol. 10, 2016, doi: [10.3389/conf.fnhum.2016.220.00001](https://doi.org/10.3389/conf.fnhum.2016.220.00001).
- [12] M. A. Klados, N. Pandria, S. Micheloyannis, D. Margulies, and P. D. Bamidis, "Math anxiety: Brain cortical network changes in anticipation of doing mathematics," *Int. J. Psychophysiol.*, vol. 122, pp. 24–31, Dec. 2017.
- [13] T. Koyama, J. G. McHaffie, P. J. Laurienti, and R. C. Coghill, "The subjective experience of pain: Where expectations become reality," *Proc. Natl. Acad. Sci. USA*, vol. 102, no. 36, pp. 12950–12955, Sep. 2005.
- [14] A. M. Owen, K. M. McMillan, A. R. Laird, and E. Bullmore, "N-back working memory paradigm: A meta-analysis of normative functional neuroimaging studies," *Hum. Brain Mapping*, vol. 25, no. 1, pp. 46–59, May 2005.
- [15] M. Hampson, N. R. Driesen, P. Skudlarski, J. C. Gore, and R. T. Constable, "Brain connectivity related to working memory performance," *J. Neurosci.*, vol. 26, no. 51, pp. 13338–13343, Dec. 2006.
- [16] D. R. Hopko, R. Mahadevan, R. L. Bare, and M. K. Hunt, "The abbreviated math anxiety scale (AMAS): Construction, validity, and reliability," *Assessment*, vol. 10, no. 2, pp. 178–182, Jun. 2003.
- [17] F. C. Richardson and R. M. Suinn, "The mathematics anxiety rating scale: Psychometric data," *J. Counseling Psychol.*, vol. 19, no. 6, pp. 551–554, 1972.
- [18] M. H. Ashcraft and A. M. Moore, "Mathematics anxiety and the affective drop in performance," *J. Psychoedu. Assessment*, vol. 27, no. 3, pp. 197–205, Jun. 2009.
- [19] S. D. Gale and D. J. Perkel, "A basal ganglia pathway drives selective auditory responses in songbird dopaminergic neurons via disinhibition," *J. Neurosci.*, vol. 30, no. 3, pp. 1027–1037, Jan. 2010.
- [20] C. D. Spielberger, R. L. Gorsuch, R. Lushene, P. R. Vagg, and G. A. Jacobs, *Manual for the State-Trait Anxiety Inventory*. Palo Alto, CA, USA: Consulting Psychologists Press, 1983.
- [21] C. D. Spielberger, "State-trait anxiety inventory," in *The Corsini Encyclopedia of Psychology*. Hoboken, NJ, USA: Wiley, 2010.
- [22] A. Delorme and S. Makeig, "EEGLAB: An open source toolbox for analysis of single-trial EEG dynamics including independent component analysis," *J. Neurosci. Methods*, vol. 134, no. 1, pp. 9–21, Mar. 2004.
- [23] M. A. Klados, C. L. Papadelis, and P. D. Bamidis, "REG-ICA: A new hybrid method for EOG artifact rejection," in *Proc. 9th Int. Conf. Inf. Technol. Appl. Biomed.*, 2009, pp. 1–4.
- [24] M. A. Klados, C. Papadelis, C. Braun, and P. D. Bamidis, "REG-ICA: A hybrid methodology combining blind source separation and regression techniques for the rejection of ocular artifacts," *Biomed. Signal Process. Control*, vol. 6, no. 3, pp. 291–300, Jul. 2011.
- [25] A. J. Bell and T. J. Sejnowski, "An information-maximization approach to blind separation and blind deconvolution," *Neural Comput.*, vol. 7, no. 6, pp. 1129–1159, 1995.
- [26] A. Schlägl, C. Keinrath, D. Zimmermann, R. Scherer, R. Leeb, and G. Pfurtscheller, "A fully automated correction method of EOG artifacts in EEG recordings," *Clin. Neurophysiol.*, vol. 118, no. 1, pp. 98–104, Jan. 2007.
- [27] W. K. Kirchner, "Age differences in short-term retention of rapidly changing information," *J. Exp. Psychol.*, vol. 55, no. 4, pp. 352–358, Apr. 1958.
- [28] F. Tadel, S. Baillet, J. C. Mosher, D. Pantazis, and R. M. Leahy, "Brainstorm: A user-friendly application for MEG/EEG analysis," *Comput. Intell. Neurosci.*, vol. 2011, 2011, Art. no. 879716, doi: [10.1155/2011/879716](https://doi.org/10.1155/2011/879716).
- [29] R. D. Pascual-Marqui, "Standardized low-resolution brain electromagnetic tomography (sLORETA): Technical details," *Methods Findings Exp. Clin. Pharmacol.*, vol. 24, pp. 5–12, Jan. 2002.
- [30] M. Kutas and K. D. Federmeier, "Thirty years and counting: Finding meaning in the N400 component of the event related brain potential (ERP)," *Annu. Rev. Psychol.*, vol. 62, pp. 621–647, Jan. 2011.
- [31] A. Heine *et al.*, "An electrophysiological investigation of non-symbolic magnitude processing: Numerical distance effects in children with and without mathematical learning disabilities," *Cortex*, vol. 49, no. 8, pp. 2162–2177, Sep. 2013.
- [32] M. Suárez-Pellicioni, M. I. Núñez-Peña, and À. Colomé, "Reactive recruitment of attentional control in math anxiety: An ERP study of numeric conflict monitoring and adaptation," *PLoS ONE*, vol. 9, no. 6, p. e99579, Jan. 2014.
- [33] I. Waisman, S. Shaul, M. Leikin, and R. Leikin, "General ability vs. expertise in mathematics: An ERP study with male adolescents who answer geometry questions," in *Proc. Electron. 12th Int. Congr. Math. Educ.*, 2012, pp. 3107–3116.
- [34] B. He, Y. Wang, and D. Wu, "Estimating cortical potentials from scalp EEGs in a realistically shaped inhomogeneous head model by means of the boundary element method," *IEEE Trans. Biomed. Eng.*, vol. 46, no. 10, pp. 1264–1268, Oct. 1999.
- [35] C. Lithari *et al.*, "Alcohol affects the brain's resting-state network in social drinkers," *PLoS ONE*, vol. 7, no. 10, p. e48641, Jan. 2012.
- [36] M. A. Klados *et al.*, "A Graph theoretical approach to study the organization of the cortical networks during different mathematical tasks," *PLoS ONE*, vol. 8, no. 8, p. e71800, Jan. 2013.
- [37] C. Lithari, M. A. Klados, C. Papadelis, C. Pappas, M. Albani, and P. D. Bamidis, "How does the metric choice affect brain functional connectivity networks?" *Biomed. Signal Process. Control*, vol. 7, no. 3, pp. 228–236, May 2012.
- [38] P. D. Welch, "The use of fast Fourier transform for the estimation of power spectra: A method based on time averaging over short, modified periodograms," *IEEE Trans. Audio Electroacoust.*, vol. 15, no. 2, pp. 70–73, Jun. 1967.
- [39] J. Saramäki, M. Kivelä, J.-P. Onnela, K. Kaski, and J. Kertész, "Generalizations of the clustering coefficient to weighted complex networks," *Phys. Rev. E, Stat. Phys. Plasmas Fluids Relat. Interdiscip. Top.*, vol. 75, no. 2, p. 027105, Feb. 2007.
- [40] J.-P. Onnela, J. Saramäki, J. Kertész, and K. Kaski, "Intensity and coherence of motifs in weighted complex networks," *Phys. Rev. E, Stat. Phys. Plasmas Fluids Relat. Interdiscip. Top.*, vol. 71, no. 6, p. 065103, Jun. 2005.
- [41] M. E. J. Newman, "Modularity and community structure in networks," *Proc. Natl. Acad. Sci. USA*, vol. 103, no. 23, pp. 8577–8582, Jun. 2006.
- [42] M. Rubinov and O. Sporns, "Complex network measures of brain connectivity: Uses and interpretations," *NeuroImage*, vol. 52, no. 3, pp. 1059–1069, Sep. 2010.
- [43] R. Guimerà, S. Mossa, A. Turtschi, and L. A. N. Amaral, "The worldwide air transportation network: Anomalous centrality, community structure, and cities' global roles," *Proc. Natl. Acad. Sci. USA*, vol. 102, no. 22, pp. 7794–7799, May 2005.
- [44] R. Guimerà and L. A. N. Amaral, "Functional cartography of complex metabolic networks," *Nature*, vol. 433, no. 7028, pp. 895–900, Feb. 2005.
- [45] U. Brandes, "A faster algorithm for betweenness centrality\*," *J. Math. Sociol.*, vol. 25, no. 2, pp. 163–177, Jun. 2001.
- [46] M. D. Humphries and K. Gurney, "Network 'small-world-ness': A quantitative method for determining canonical network equivalence," *PLoS ONE*, vol. 3, no. 4, p. e0002051, Jan. 2008.
- [47] A. Zalesky, A. Fornito, and E. T. Bullmore, "Network-based statistic: Identifying differences in brain networks," *NeuroImage*, vol. 53, no. 4, pp. 1197–1207, Dec. 2010.
- [48] D. R. Hopko, D. W. McNeil, C. W. Lejuez, M. H. Ashcraft, G. H. Eifert, and J. Riel, "The effects of anxious responding on mental arithmetic and lexical decision task performance," *J. Anxiety Disorders*, vol. 17, no. 6, pp. 647–665, 2003.

- [49] N. Tzourio-Mazoyer *et al.*, "Automated anatomical labeling of activations in SPM using a macroscopic anatomical parcellation of the MNI MRI single-subject brain," *NeuroImage*, vol. 15, no. 1, pp. 273–289, Jan. 2002.
- [50] W. Klimesch, "Alpha-band oscillations, attention, and controlled access to stored information," *Trends Cogn. Sci.*, vol. 16, no. 12, pp. 606–617, Dec. 2012.
- [51] M. Siegel, M. R. Warden, and E. K. Miller, "Phase-dependent neuronal coding of objects in short-term memory," *Proc. Nat. Acad. Sci. USA*, vol. 106, no. 50, pp. 21341–21346, Dec. 2009.
- [52] A. K. Engel and P. Fries, "Beta-band oscillations—Signalling the status quo?" *Curr. Opin. Neurobiol.*, vol. 20, no. 2, pp. 156–165, Apr. 2010.
- [53] S. E. Petersen and M. I. Posner, "The attention system of the human brain: 20 years after," *Annu. Rev. Neurosci.*, vol. 35, pp. 73–89, Jan. 2012.
- [54] M. R. Delgado, K. I. Nearing, J. E. Ledoux, and E. A. Phelps, "Neural circuitry underlying the regulation of conditioned fear and its relation to extinction," *Neuron*, vol. 59, no. 5, pp. 829–838, Sep. 2008.
- [55] A. Etkin, T. Egner, and R. Kalisch, "Emotional processing in anterior cingulate and medial prefrontal cortex," *Trends Cogn. Sci.*, vol. 15, no. 2, pp. 85–93, Feb. 2011.
- [56] C. Büchel, K. Bornhövd, M. Quante, V. Glauche, B. Bromm, and C. Weiller, "Dissociable neural responses related to pain intensity, stimulus intensity, and stimulus awareness within the anterior cingulate cortex: A parametric single-trial laser functional magnetic resonance imaging study," *J. Neurosci.*, vol. 22, no. 3, pp. 970–976, Feb. 2002.
- [57] Y. Oshiro, A. S. Quevedo, J. G. McHaffie, R. A. Kraft, and R. C. Coghill, "Brain mechanisms supporting discrimination of sensory features of pain: A new model," *J. Neurosci.*, vol. 29, no. 47, pp. 14924–14931, Nov. 2009.
- [58] C. J. Starr *et al.*, "Roles of the insular cortex in the modulation of pain: Insights from brain lesions," *J. Neurosci.*, vol. 29, no. 9, pp. 2684–2694, Mar. 2009.
- [59] F. Zeidan, K. T. Martucci, R. A. Kraft, N. S. Gordon, J. G. McHaffie, and R. C. Coghill, "Brain mechanisms supporting modulation of pain by mindfulness meditation," *J. Neurosci.*, vol. 31, no. 14, pp. 5540–5548, Apr. 2011.
- [60] K. Nader, G. E. Schafe, and J. E. Le Doux, "Fear memories require protein synthesis in the amygdala for reconsolidation after retrieval," *Nature*, vol. 406, no. 6797, pp. 722–726, Aug. 2000.
- [61] C. Styliadis, A. A. Ioannides, P. D. Bamidis, and C. Papadelis, "Amygdala responses to valence and its interaction by arousal revealed by MEG," *Int. J. Psychophysiol.*, vol. 93, no. 1, pp. 121–133, Jul. 2014.
- [62] E. J. Mufson, M. M. Mesulam, and D. N. Pandya, "Insular interconnections with the amygdala in the rhesus monkey," *Neuroscience*, vol. 6, no. 7, pp. 1231–1248, Jan. 1981.
- [63] D. P. Friedman, E. A. Murray, J. B. O'Neill, and M. Mishkin, "Cortical connections of the somatosensory fields of the lateral sulcus of macaques: Evidence for a corticolimbic pathway for touch," *J. Comp. Neurol.*, vol. 252, no. 3, pp. 323–347, Oct. 1986.
- [64] B. A. Vogt and D. N. Pandya, "Cingulate cortex of the rhesus monkey: II. Cortical afferents," *J. Comp. Neurol.*, vol. 262, no. 2, pp. 271–289, Aug. 1987.
- [65] A. P. R. Smith, R. N. A. Henson, R. J. Dolan, and M. D. Rugg, "fMRI correlates of the episodic retrieval of emotional contexts," *NeuroImage*, vol. 22, no. 2, pp. 868–878, Jun. 2004.
- [66] A. Baddeley, "Working memory: Looking back and looking forward," *Nat. Rev. Neurosci.*, vol. 4, no. 10, pp. 829–839, Oct. 2003.
- [67] C. Ranganath, M. K. Johnson, and M. D'Esposito, "Prefrontal activity associated with working memory and episodic long-term memory," *Neuropsychologia*, vol. 41, no. 3, pp. 378–389, Jan. 2003.
- [68] M. Toepper *et al.*, "Hippocampal involvement in working memory encoding of changing locations: An fMRI study," *Brain Res.*, vol. 1354, pp. 9–91, Oct. 2010.
- [69] C. C. Faraco *et al.*, "Complex span tasks and hippocampal recruitment during working memory," *NeuroImage*, vol. 55, no. 2, pp. 773–787, Mar. 2011.
- [70] D. D. Jolles, M. J. Grol, M. A. Van Buchem, S. A. Rombouts, and E. A. Crone, "Practice effects in the brain: Changes in cerebral activation after working memory practice depend on task demands," *NeuroImage*, vol. 52, no. 2, pp. 658–668, Aug. 2010.
- [71] B. A. Kirchhoff, A. D. Wagner, A. Maril, and C. E. Stern, "Prefrontal-temporal circuitry for episodic encoding and subsequent memory," *J. Neurosci.*, vol. 20, no. 16, pp. 6173–6180, Aug. 2000.
- [72] S. Y. Bookheimer, T. A. Zeffiro, T. Blaxton, W. Gaillard, and W. Theodore, "Regional cerebral blood flow during object naming and word reading," *Hum. Brain Mapping*, vol. 3, no. 2, pp. 93–106, Oct. 1995.
- [73] J. D. Cohen *et al.*, "Temporal dynamics of brain activation during a working memory task," *Nature*, vol. 386, no. 6625, pp. 604–608, Apr. 1997.
- [74] I. Deschamps, S. R. Baum, and V. L. Gracco, "On the role of the supramarginal gyrus in phonological processing and verbal working memory: Evidence from rTMS studies," *Neuropsychologia*, vol. 53, pp. 39–46, Jan. 2014.
- [75] J. H. Callicott *et al.*, "Physiological characteristics of capacity constraints in working memory as revealed by functional MRI," *Cerebral Cortex*, vol. 9, no. 1, pp. 6–20, 1999.
- [76] N. J. Cohen, R. A. Poldrack, and H. Eichenbaum, "Memory for items and memory for relations in the procedural/declarative memory framework," *Memory*, vol. 5, nos. 1–2, pp. 131–178, 1997.
- [77] B. Rypma, V. Prabhakaran, J. E. Desmond, G. H. Glover, and J. D. E. Gabrieli, "Load-dependent roles of frontal brain regions in the maintenance of working memory," *NeuroImage*, vol. 9, no. 2, pp. 216–226, Feb. 1999.
- [78] A. F. T. Arnsten, "The biology of being frazzled," *Science*, vol. 280, no. 5370, pp. 1711–1712, Jun. 1998.
- [79] S. Qin, E. J. Hermans, H. J. F. van Marle, J. Luo, and G. Fernández, "Acute psychological stress reduces working memory-related activity in the dorsolateral prefrontal cortex," *Biol. Psychiatry*, vol. 66, no. 1, pp. 25–32, Jul. 2009.
- [80] C. Liston, B. S. McEwen, and B. J. Casey, "Psychosocial stress reversibly disrupts prefrontal processing and attentional control," *Proc. Nat. Acad. Sci. USA*, vol. 106, no. 3, pp. 912–917, Jan. 2009.
- [81] S. I. Dimitriadis, N. A. Laskaris, V. Tsirka, M. Vourkas, and S. Micheloyannis, "What does delta band tell us about cognitive processes: A mental calculation study," *Neurosci. Lett.*, vol. 483, no. 1, pp. 11–15, 2010.
- [82] J. N. Frey, N. Mainy, J.-P. Lachaux, N. Müller, O. Bertrand, and N. Weisz, "Selective modulation of auditory cortical alpha activity in an audiovisual spatial attention task," *J. Neurosci.*, vol. 34, no. 19, pp. 6634–6639, May 2014.
- [83] P. Manza, C. L. Hau, and H. C. Leung, "Alpha power gates relevant information during working memory updating," *J. Neurosci.*, vol. 34, no. 17, pp. 5998–6002, Apr. 2014.
- [84] B. Spitzer, S. Fleck, and F. Blankenburg, "Parametric alpha- and beta-band signatures of supramodal numerosity information in human working memory," *J. Neurosci.*, vol. 34, no. 12, pp. 4293–4302, Mar. 2014.
- [85] I. M. Lyons and S. L. Beilock, "Mathematics anxiety: Separating the math from the anxiety," *Cereb. Cortex*, vol. 22, no. 9, pp. 2102–2110, Sep. 2012.



**MANOUSOS A. KLADOS** (M'17) received the B.Sc. degree in mathematics, the M.Sc. degree (Hons.) in medical informatics, and the Ph.D. degree (Hons.) in medicine from the Aristotle University of Thessaloniki, in 2007, 2009, and 2014, respectively. He was Postdoctoral Fellow with the Neuroanatomy and Connectivity research Group, Max Planck Institute for Human Cognitive and Brain Science, from 2014 to 2016, and a Senior Researcher with the Chair of Lifespan Development Neurosciences, Technical University of Dresden. He is currently a Lecturer with the Department of Biomedical Engineering, Aston University. He has authored 25 journal articles and more than 30 contributions in international conferences with posters and talks. His research interests include mathematical anxiety, brain networks, affective and personality computing, and biomedical signal processing. He received several prizes and scholarships for his research excellence. He chaired one international conference (SAN2016). He was on the organization/international committee of several conferences. He is currently the Coordinator of the large EU Project funded by the H2020-MC-RISE Scheme and Co-PI of the Knowledge Transfer Partnership.



**EVANGELOS PARASKEVOPOULOS** received the bachelor's and master's degrees from the Psychology Department, Aristotle University of Thessaloniki (A.U.TH.), the Music Diploma degree in harmony, counterpoint, and fugue by studying music theory, and the Ph.D. degree (*summa cum laude*) in cognitive neurosciences and magnetoencephalography with the Institute for Biomagnetism and Biosignalanalysis, Münster, Germany, in 2013, under the supervision of Prof. Dr. C. Pantev. He is currently a Postdoctoral Research Associate with the Laboratory of Medical Physics, A.U.TH., and a part-time Lecturer with the Psychology Department, City College, The University of Sheffield. He has more than 20 published papers in international refereed journals, three book chapters, and more than 35 contributions in international conferences with posters and talks. His research interests include cortical plasticity, music perception (disorders), and multisensory integration. In 2011, he received the Award in the Young Neuroscientist Poster Competition NeuroVisionen 8 from the NeuroNRW—Ministry of Innovation, Science and Research of the State of North Rhine-Westphalia, Germany, and the Postdoctoral Research Fellowship from A.U.TH. (Excellence). In 2017, he received a Postdoctoral Research Fellowship from the Foundation of State Fellowships of Greece (IKY) and, in 2018, a Postdoctoral Research Grant from ELIDEK.



**PANAGIOTIS D. BAMIDIS** (M'09) received the Diploma degree in physics from the Aristotle University of Thessaloniki (AUTH), Thessaloniki, Greece, in 1990, the M.Sc. degree (Hons.) in medical physics from the University of Surrey, Guildford, U.K., in 1992, and the Ph.D. degree in bioelectromagnetism and functional brain analysis and imaging from The Open University, Milton Keynes, U.K., in 1996. He is currently an Associate Professor of medical education informatics with the Laboratory of Medical Physics, Medical School, AUTH. He has been a coordinator of large European projects ([www.longlastingmemories.eu](http://www.longlastingmemories.eu); [www.mediator.net](http://www.mediator.net); [www.epblnet.eu](http://www.epblnet.eu); [www.smokefreebrain](http://www.smokefreebrain); and [www.childrenhealth.eu](http://www.childrenhealth.eu)) and the Principal Investigator for a number of national and international funded projects (more than 40 in total). His research interests include assistive technologies (silver science, silver gaming, mobile health, decision support, and avatars), technology-enhanced learning in medical education (web2.0, semantic web, serious games, virtual patients, problem-based learning, and learning analytics), and affective and physiological computing and human-computer interaction, (bio)medical informatics with an emphasis on neurophysiological sensing and health information management (open-health big data), and affective neurosciences. He is a member of the Advisory Board for the Open Knowledge Foundation (OKFN), a Founding Member of the OKFN Greek Chapter, and the President of the Greek Biomedical Technology Society and the Society of Applied Neuroscience. He received the Prize of the AUTH Research Committee for the Best Track Record in funded research projects among AUTH Young Academic Staff, in 2009. He has been the Chairman/Organizer of seven international conferences (iSHIMR2001, iSHIMR2005, MEDICON2010, GASMA2010, SAN2011, MEI2012, and MEI2015) and the Conference Producer of the Medical Education Informatics Conference and the Spring/Summer School Series.



**NIKI PANDRIA** the bachelor's degree and the M.Sc. degree (Hons.) in statistics and modeling, under the supervision of Associate Professor D. Kugiumtzis, from the Department of Mathematics, Aristotle University of Thessaloniki (AUTH), in 2011 and 2013, respectively, where she is currently pursuing the Ph.D. degree, under the supervision of Associate Professor P. Bamidis, with the Medical Physics Laboratory, Medical School. Her Ph.D. thesis is on neuroscientific investigation of addiction and the role of neurofeedback. Since 2013, she has been a Research Associate with the Medical Physics Laboratory, Medical School, AUTH, under the supervision of Associate Professor P. Bamidis. She is a member of the Neuroscience of Cognition and Affection Group, hosted in the Laboratory of Medical Physics, and the Hellenic Mathematical Association. She is certified as a Neurofeedback Trainer by the IFEN Institute. She has contributions in interdisciplinary conferences either as presenter or having poster presentations. She is the author of scientific papers. Her research interests include Neurofeedback's applications, the study of brain networks using graph theory and the correlation of time series. She received a scholarship for her performance during M.Sc. degree.